# Carbon Nanotube-promoted Co-Cu Catalyst for Highly Efficient Synthesis of Higher Alcohols from Syngas

Hong-Bin Zhang[*], Xin Dong, Guo-Dong Lin, Xue-Lian Liang, Hai-Yan Li

Supporting Information

MWCNT preparation

CNTs were prepared following the method reported previously.[15] The freshly prepared CNTs were treated with boiling nitric acid, followed by rinsing with de-ionized water, then drying under dry nitrogen. Open-end CNTs with somewhat hydrophilic surface were then obtained. TEM image of such homemade CNTs is shown in Figure 1a.

(a)   **(b)**
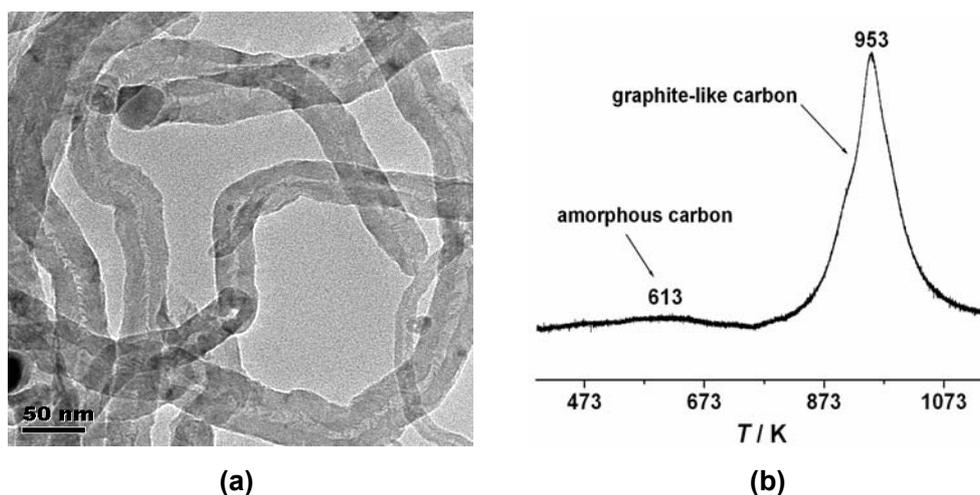
Fig. 1 TEM image (a) (taken by a FEI–F30 electron microscope) and H_2-TPH spectrum (b) of the purified CNTs.

Previous characterization studies [15,16] have shown that this type of CNTs was a "Herringbone-type" MWCNTs, with the outer diameters of 10~50 nm, inner diameters at 3~5 nm, and N_2-BET surface area at ~140 $m^2 \cdot g^{-1}$. Their main XRD feature was close to that of graphite, but somewhat broadened, implying that the degree of long-range order of these nanostructures was relatively low compared to that of graphite. HRTEM images revealed that these CNTs were constructed by a superposition of many graphene layer facets, tilted at a certain angle with respect to the axis of the central hollow nanofibre. H_2-temperature-programmed hydrogenation (H_2-TPH) measurement

---

* E-mail address: hbzhang@xmu.edu.cn

showed that the carbon nanostructures in the purified CNTs were predominantly graphite-like, and the content of amorphous carbon was very low ($\leq 10wt\%$) (Figure 1b). Moreover, the H_2-TPH result also showed that this type of CNTs was stable in H_2-atmosphere at temperatures below 773 K.

Catalyst preparation

Using the above home-made CNTs and the nitrates of the corresponding metallic components, a series of CNT-promoted Co-Cu catalysts, denoted as Co_iCu_j-$x\%$(mass %)CNTs, were prepared by constant-pH co-precipitation method [R. G. Herman, K. Klier, G. W. Simmons, B. P. Finn, J. B. Bulko, T. P. Kobylinski, *J. Catal.,* 1979, **56**, 407-429]. An aqueous solution containing calculated amounts of Co and Cu (total equivalent concentration of metallic cations at 4 N), which was prepared by dissolving $Co(NO_3)_2\cdot6H_2O$ and $Cu(NO_3)_2\cdot3H_2O$ (all of AR grade) in deionized water, and an aqueous K_2CO_3 solution (4 N) were simultaneously added drop-wise under vigorous stirring into a Pyrex flask containing a calculated amount of the HNO_3-treated CNTs at constant temperature of 353 K. The addition was adjusted to maintain a constant pH at ~7. The precipitation procedure was completed in 1 h. The precipitate was then continuously stirred for 5 h under the temperature of 353 K, followed by aging overnight at room temperature and then filtering. It was then rinsed several times with deionized water until the content of K^+ ions in the eluant fell below 0.1 ppm as detected by flame ion absorption method. The precipitate was then dried at 393 K for 4 h and calcined at 543~573 K for 3 h to yield the precursor of CNT-promoted Co-Cu catalysts. A CNT-free conventional co-precipitated Co-Cu catalyst, used as reference, was prepared in the similar way. All samples of catalyst precursor were pressed, crushed, and sieved to a size of 40~80 mesh for the activity evaluation.

Catalyst evaluation

The catalyst was tested for synthesis of the higher alcohols in a continuous-flow micro-reactor-GC combination system. 0.50 g of catalyst (equivalent to ~0.5 mL of catalyst sample) was used for each test. Prior to the reaction, catalyst sample was pre-reduced by $5\%H_2+N_2$ for 16 h. Synthesis of the higher alcohols from syngas over the catalysts was conducted at a stationary state with premixed feed gas composition of $H_2/CO/CO_2/N_2 = 46/46/5/3$ (v/v) under 523~583 K, 5.0 MPa. The reactants and products were determined by an on-line GC (Model GC-950) equipped with dual detectors (TCD and FID) and dual columns filled with carbon molecular sieve (TDX-01) and Porapak Q-S, respectively. The former column was used for analysis of CO, CH_4, N_2 (as internal standard) and CO_2, and the latter for CO/N_2, $C_{1\sim4}$-alkanes, $C_{1\sim4}$-alcohols and other oxygenates. The data were all taken 120 minutes after the reaction started and a stationary activity appeared. CO conversion was

determined through an internal standard, and the carbon-based selectivity of the carbon-containing products (including alcohols, alkanes, and other oxygenates) was calculated by an internal normalization method.

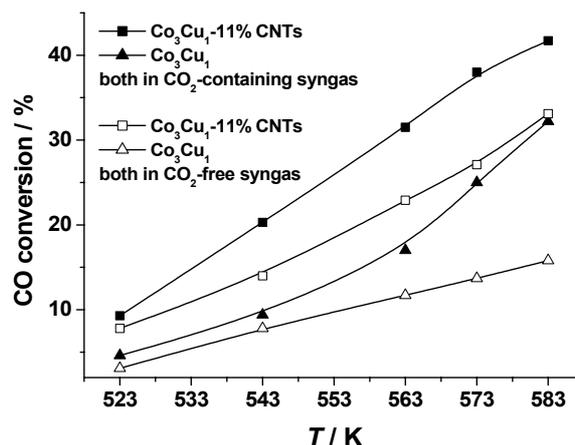*The effect of CO$_2$ additive in the feed syngas on the conversion of CO hydrogenation:*

Fig.2 Reaction activity of the higher alcohol synthesis over the Co$_3$Cu$_1$-x%CNTs catalysts fed with CO$_2$-containing or CO$_2$-free feed gas: V(H$_2$)/V(CO)/V(CO$_2$)/V(N$_2$) = 46/46/5/3 or V(H$_2$)/V(CO)/V(N$_2$) = 45/45/10, all at 5.0 MPa, GHSV = 10000 mL(STP) h^{-1} g$_{-cat.}$$^{-1}$

Selectivity of CO hydrogenation-conversion to form alcohols, alkanes, CO$_2$ over the CNT-free Co$_3$Cu$_1$ catalyst fed with the CO$_2$-free syngas
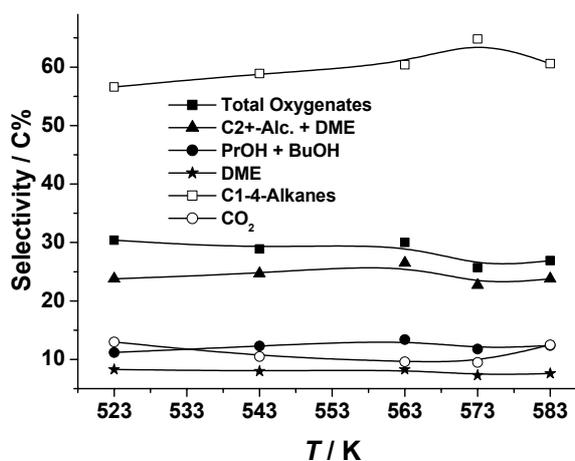

Fig. 3 Dependence of selectivity of products in the alcohol synthesis upon temperature over the CNT-free catalyst, Co$_3$Cu$_1$, at 5.0 MPa, H$_2$/CO/N$_2$ = 45/45/10 (v/v), GHSV= 10000 mL(STP)•h^{-1}•g$_{-cat.}$$^{-1}$.

Table 1
Comparison of selectivities of higher alcohol synthesis over the Co_3Cu_1-11%CNTs catalysts vs. its CNT-free counterpart, Co_3Cu_1, fed with the CO_2-containing syngas vs. CO_2-free syngas.

Catalyst	Feed gas	CO conv. / %	Selectivity / C%							
			$C_{1\sim4}$-Oxygenates	$C_{1\sim4}$-Alkanes	CO_2	BuOH	DME	PrOH	EtOH	MeOH
Co_3Cu_1-11%CNTs	*5%CO_2-containing	38.0	70.5	28.0	1.4	45.0	14.8	5.1	2.7	1.1
	**CO_2-free	27.1	42.4	50.3	7.3	7.4	14.6	8.5	7.7	3.4
Co_3Cu_1-0%CNTs	*5%CO_2-containing	25.3	63.9	33.1	3.0	22.6	20.1	9.9	3.4	7.4
	**CO_2-free	13.7	25.7	64.8	9.5	5.0	7.3	6.8	3.6	2.4

Reaction condition: 5.0 MPa, 573 K, *$H_2/CO/CO_2/N_2$ = 46/46/5/3 (v/v) or ** $H_2/CO/N_2$ = 45/45/10 (v/v), GHSV= 10000 mL(STP)$\bullet h^{-1} \bullet g_{cat.}^{-1}$.

Table 2
STY of products in the HAS over the Co_3Cu_1-x%CNTs catalysts*

Catalyst	T / K	Specific reaction rate/mmol-CO$\bullet h^{-1} \bullet$ (g-Co_3Cu_1)$^{-1}$	STY / mg$\bullet h^{-1} \bullet g_{cat.}^{-1}$				
			BuOH	DME	$C_{2\sim4}$-OH + DME	$C_{1\sim4}$ oxygenates	$C_{1\sim4}$ alkanes
Co_3Cu_1-11%CNTs	563	72.69	533	221	899	908	268
	573	87.69	649	265	1042	1102	328
	583	96.22	562	338	1075	1156	427
Co_3Cu_1-0%CNTs	563	33.47	135	149	385	441	170
	573	51.96	223	241	609	731	258
	583	66.95	230	257	759	841	386

*at: 5.0 MPa, $H_2/CO/CO_2/N_2$= 46/46/5/3(v/v), GHSV= 10000 mL(STP)$\bullet h^{-1} \bullet g_{cat.}^{-1}$.

The apparent activation energy of conversion of CO hydrogenation

The apparent activation energy was measured between 523 and 583 K at the reaction conditions of 2.0 MPa, $H_2/CO/CO_2/N_2$=62/30/5/3(v/v), GHSV= 12000 mL-h^{-1}-$g_{cat.}^{-1}$, with CO conversion at between 1%~12%. The results are illustrated in the Arrhenius plot in Fig. 4. The apparent activation energy for the hydrogenation-conversion of CO on the Co_3Cu_1-11%CNTs catalyst was found to be

10.7 Kcal•mol^{-1}. This value is somewhat lower than that (12.2 Kcal•mol^{-1}) on the corresponding CNT-free counterpart.
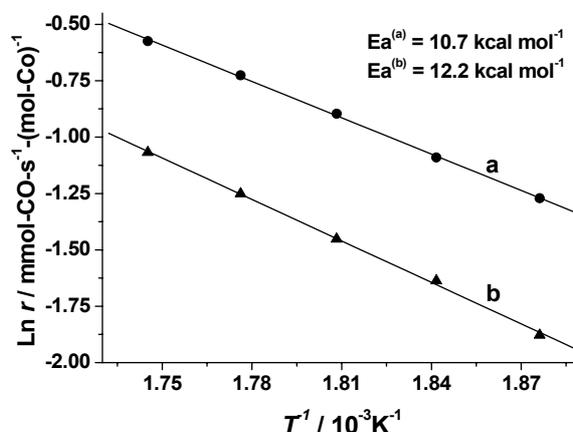

Fig. 4 Arrhenius plots of the higher alcohol synthesis over (a) Co$_3$Cu$_1$-11%CNTs and (b) Co$_3$Cu$_1$, at: 2.0 MPa, 523~583 K, H$_2$/CO/CO$_2$/N$_2$=62/30/5/3(v/v), GHSV= 12000 mL(STP)•h^{-1}•g$_{-cat.}$$^{-1}$.

Catalyst characterization

BET specific surface area (SSA) of the CNT sample and the catalyst precursors was measured by N$_2$ adsorption using a Micromeritics Tristar-3000 (Carlo Erba, USA) system. TEM observation of CNTs was performed by a FEI–F30 or JEM 100CX- electron microscope. X-ray diffraction measurements were carried out on a Rigaku Rotaflex D/Max-C X-ray Diffractometer with Cu-K$_\alpha$ radiation at a scanning rate of 8°•min^{-1}. XPS measurements were done on a VG ESCA LAB MK-2 system with Mg-K$_\alpha$ radiation (10 kV, 20 mA, hv = 1253.6 eV) under UHV (1×10^{-7} Pa), calibrated internally by the carbon deposit C(1s) (B.E.) at 284.6 eV.

Tests of H$_2$-TPR and H$_2$-TPD of catalyst were conducted on a fixed-bed continuous-flow reactor or adsorption-desorption system. A KOH-column and a 3A-zeolite molecular sieve column were installed in sequence at the reactor-exit to remove water vapor produced by the reduction of metallic oxide components of the catalyst sample. The rate of temperature increase was 10 K•min^{-1}. Change of hydrogen-signal was monitored using an on-line GC (Shimadzu GC-8A) with a TC detector. For TPR measurement, 20 mg of catalyst precursor in oxidation state was used for each test. The sample was first flushed by an Ar (of 99.999% purity) stream at 673 K for 30 minutes to clean its surface, and then cooled down to room temperature, followed by switching to a N$_2$-carried 5v% H$_2$ gaseous mixture as reducing gas to start the TPR measurement. For TPD test, 100 mg of catalyst sample was used each time. Prior to TPD test, the catalyst sample was pre-reduced *in-situ*

in the TPD equipment by a N_2-carried $5v\%H_2$ gaseous mixture, with the highest reduction-temperature reaching 523 K and lasting 16 h. Shortly after, the reduced sample was cooled to 433 K, followed by switching to a H_2 (of 99.999% purity) stream and maintaining at that temperature for 30 min, subsequently cooling down to room temperature and maintaining at room temperature for 1 h, and then flushing by a Ar (of 99.999% purity) stream at room temperature till the stable baseline of GC appeared.

H_2-TPR test of the oxidized precursor of the catalysts

It was found by H_2-TPR test that appropriate incorporation of a minor amount of CNTs into the Co_3Cu_1 led to lowering in its reduction-temperature (Figure 5), simultaneously increasing the Co_xCu_y species reducible to lower valence-state(s) in the total Co_3Cu_1 amount. As estimated from Figure 5a vs. 5b, the total area-intensity of the H_2-TPR peaks in the range of 373~623 K (corresponding to a certain H_2-consumed amount) was increased by 12% due to the addition of CNTs. Considering that the ratio of Co_3Cu_1 content in the CNT-promoted system vs. that in the CNT-free counterpart was 89% vs. 100% (mass percentage), it could be estimated that the amount of hydrogen consumed by unit mass of Co_3Cu_1 of the CNT-promoted system was 1.25 times that of its CNT-free counterpart.
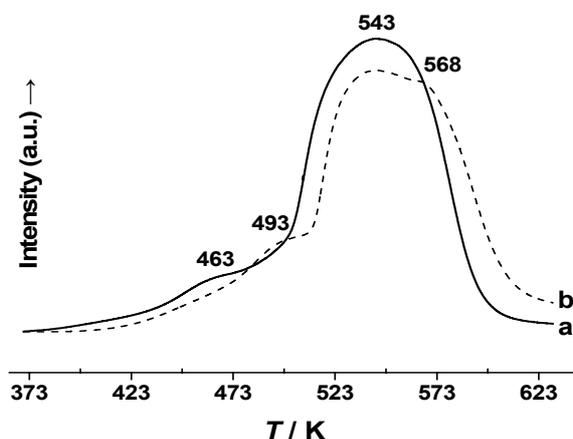

Fig. 5 H_2-TPR spectra of the oxidized precursor of catalyst: (a) Co_3Cu_1-11%CNTs and (b) Co_3Cu_1.

XRD patterns of the functioning catalysts

The XRD patterns (Fig. 6) of the two catalysts undergoing 6 h of the reaction operation for the HAS showed that the Co-Cu components existed mainly in the forms of CoCu-alloy and divided metallic Cu_y^0, and that the presence of divided metallic Co_x^0-phase could not be excluded.

Moreover, the content level of either Co-Cu spinel or Co_3O_4 phase was extremely low, especially in the CNT-promoted system. This implied that the reduction of the CNT-promoted catalyst was more complete, in line with the above H_2-TPR results. According to the well-known Scherrer's equation, it may be estimated from the half-peak width of the peaks at $2\theta = 51.1°$ and $75.5°$ that the particle size of divided metallic Cu_x^0-crystallites was about 8 nm. Considering that the main XRD peak centred at $2\theta = 44.0°$ may contain the contribution from CoCu-alloy phase, divided metallic Cu_y^0 and Co_x^0-phases, the size of each type of the crystallites can not be estimated from the half-peak width of the main peaks at $2\theta = 44.0°$.

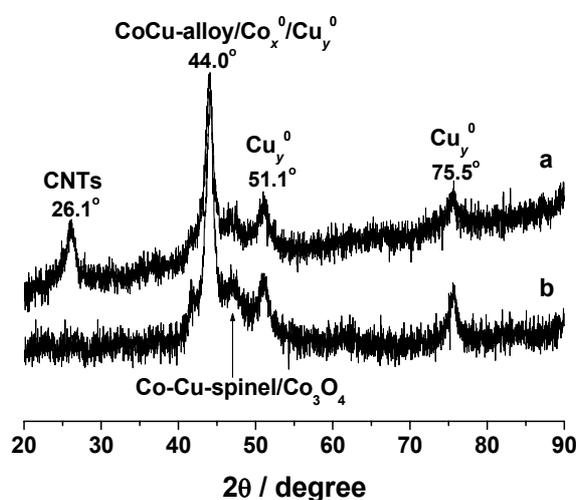Fig. 6 XRD patterns of the functioning catalysts: (a) Co_3Cu_1-11%CNTs; (b) Co_3Cu_1.

Behaviour of adsorption/desorption of H_2 on the reduced catalysts

In recent years there has been considerable experimental and theoretical interest in the use of nanostructured carbon materials as potential hydrogen sorbents. It was demonstrated by Ishikawa et al. [In: *Chemistry and Physics of Carbon,* Walker, P. L. Jr.; Thrower, P. A.; Eds. Marcel Dekker, New York, 1975; Vol. **12**, p.39] that graphitized carbon black surfaces were capable of rapidly equilibrating H_2/D_2 mixture. A dissociation rate of 2.5×10^{17} molecules s^{-1} $(m^2\text{-ASA})^{-1}$ (ASA – active surface area) was measured at ambient temperatures and pressures, irrespective of the nature of the carbon material under investigation. The ASA was described in terms of atoms located at edge positions on the graphite basal plane and was determined from the amount of oxygen able to chemisorb at these sites.

Our recent H_2-TPD investigation [Zhou, Z. H. et al. *Acta Phys.-Chim. Sinica* **18** (2002) 692] showed that hydrogen adsorption on the CNTs can occur at room temperature and atmospheric pressure and that the desorbed product was almost exclusively gaseous hydrogen at temperatures lower than ~693 K, and involved CH_4, C_2H_4 and C_2H_2, in addition to H_2, at temperatures of 693 K and above, implying that H_2 adsorption on the CNTs may be in the two forms: associative (molecular state) and dissociative (atomic state). This has been also demonstrated by our LRS characterization of H_2/MWCNTs adsorption system [Zhang, H. B., et al. *Carbon* **40** (13) (2002) 2429].

The Figure 7 (i.e. Figure 4 in the revised manuscript) showed the TPD spectra taken on the pre-reduced catalysts adsorbing H_2 (99.999% purity) at 433 K followed by cooling down to room temperature. On the CNT-promoted system, the observed H_2-desorption peaks were present at 418 K (peak-I), 523 K (peak-II, a shoulder) and 873 K (peak-III). The peaks I and II originated from desorption of the hydrogen-species adsorbed weakly or medium-strongly, while the peak III was due to the desorption of hydrogen-species adsorbed strongly, most probably dissociatively chemisorbed hydrogen H(a). For the CNT-free reference system, the observed H_2-desorption was mainly at peak-I, while the H_2-desorption intensity in the temperature region of the above peaks II and III was extremely low. The relative area-intensities of peaks Is, IIs and IIIs for these catalyst samples were estimated, and the results were listed in Table 3.
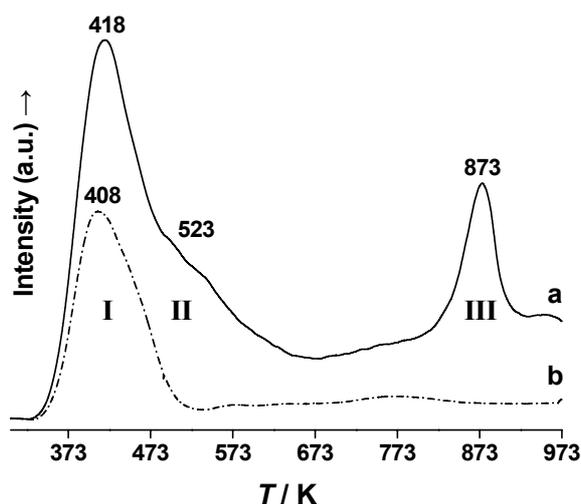

Fig. 7 H_2-TPD spectra of the pre-reduced catalysts: (a) Co_3Cu_1-11%CNTs and (b) Co_3Cu_1.

Table 3
Relative area-intensity of H_2-TPD peaks I, II and II for the pre-reduced catalysts

Catalyst sample	Relative area-intensity*		
	Peak I	Peak II	Peak III
Co_3Cu_1-11%CNTs	100	41	31
Co_3Cu_1	54	5	4

*With area-intensity of the strongest peak I as 100.

TEM images of the functioning catalysts

Figure 8 showed TEM images of the CNT-promoted catalyst and its CNT-free counterpart both undergoing 3 h of the reaction operation for the HAS.
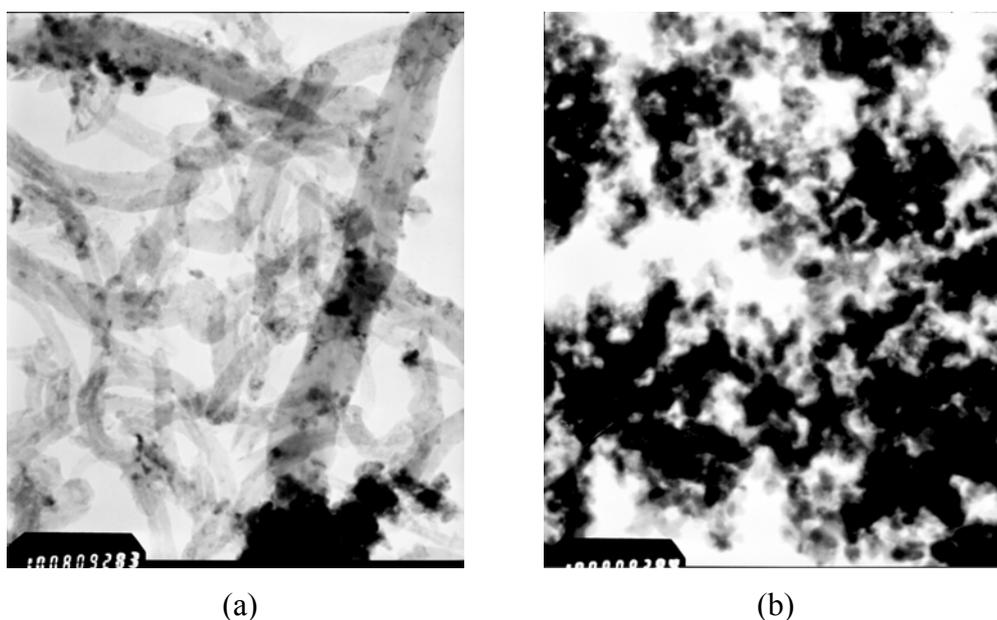

(a)   (b)

Fig. 8 TEM images of the functioning catalysts: (a) Co_3Cu_1-11%CNTs and (b) Co_3Cu_1, both undergoing 3 h of the reaction operation for the HAS   taken by JEM 100CX-   electron microscope

The above TEM images showed that, the CNT-free catalyst mainly contained CoCu alloy of various sizes, as well as divided Cu_x^0 and Co_y^0 particles, while the CNT-promoted catalyst contained CNTs with the alloy and/or divided metal species deposited on the surface, in addition to CoCu alloy and/or the divided metal crystallites of various sizes. Note that not all alloy/metal crystallites were highly dispersed on the surface of CNTs, because the doping amount of CNTs was only 11wt%. This also implied that hydrogen-spillover played an important role in promoting this reaction.

Cu(2p)-XPS-spectra of the functioning catalysts

Cu(2p)-XPS of the functioning Co_3Cu_1-11%CNTs catalyst and its CNT-free counterpart was shown in Figure 9. It can be seen that little difference in valence of the surface Cu-species existed between the functioning Co_3Cu_1-11%CNTs catalyst and its CNT-free counterpart, Co_3Cu_1. The observed surface Cu-species all are in Cu^0, with $Cu^0(2p_{3/2}) = 932.6$ eV(B.E.) and $Cu^0(2p_{1/2}) = 952.6$ eV(B.E.).
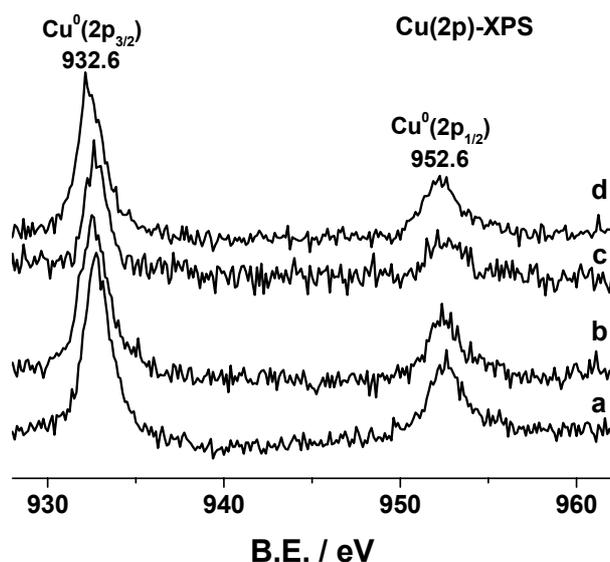

Fig. 9 Cu(2p)-XPS-spectra of the functioning catalysts: (a) Co_3Cu_1 and (b) Co_3Cu_1-11%CNTs, both fed with the CO_2-containing syngas: $H_2/CO/CO_2/N_2 = 46/46/5/3$ (v/v); (c) Co_3Cu_1 and (d) Co_3Cu_1-11%CNTs, both fed with the CO_2-free syngas: $H_2/CO//N_2 = 45/45/10$ (v/v).